JACC: CARDIOVASCULAR IMAGING VOL. 8, NO. 1, 2015

ISSN 1936-878X/$36.00
PUBLISHED BY ELSEVIER INC. http://dx.doi.org/10.1016/j.jcmg.2014.08.012

iCONCEPTS

CONCEPTS ON THE VERGE OF TRANSLATION

Association of Myocardial T1-Mapping CMR With Hemodynamics and RV Performance in Pulmonary Hypertension

Ana García-Álvarez, MD, PhD,*†‡ Inés García-Lunar, MD,*†§ Daniel Pereda, MD,*†‡ Rodrigo Fernández-Jimenez, MD,*†‖ Javier Sánchez-González, PhD,*†¶ Jesús G. Mirelis, MD, PhD,*†# Mario Nuño-Ayala, PhD,*† Damian Sánchez-Quintana, MD,** Leticia Fernández-Friera, MD, PhD,*††† Jose M. García-Ruiz, MD,*†‡‡ Gonzalo Pizarro, MD,*†§ Jaume Agüero, MD,*† Paula Campelos, MD,‡ Manuel Castellá, MD, PhD,‡ Manel Sabaté, MD, PhD,‡ Valentin Fuster, MD, PhD,†§§ Javier Sanz, MD,§§ Borja Ibañez, MD, PhD*†‖

ABSTRACT

Early detection of right ventricular (RV) involvement in chronic pulmonary hypertension (PH) is essential due to prognostic implications. T1 mapping by cardiac magnetic resonance (CMR) has emerged as a noninvasive technique for extracellular volume fraction (ECV) quantification. We assessed the association of myocardial native T1 time and equilibrium contrast ECV (Eq-ECV) at the RV insertion points with pulmonary hemodynamics and RV performance in an experimental model of chronic PH. Right heart catheterization followed by immediate CMR was performed on 38 pigs with chronic PH (generated by surgical pulmonary vein banding) and 6 sham-operated controls. Native T1 and Eq-ECV values at the RV insertion points were both significantly higher in banded animals than in controls and showed significant correlation with pulmonary hemodynamics, RV arterial coupling, and RV performance. Eq-ECV values also increased before overt RV systolic dysfunction, offering potential for the early detection of myocardial involvement in chronic PH. (J Am Coll Cardiol Img 2015;8:76–82) © 2015 by the American College of Cardiology Foundation.

Right ventricular (RV) performance is the main determinant of morbidity and mortality in chronic pulmonary hypertension (PH). There is consequently great interest in developing tools that allow early detection of RV involvement in patients with PH. Cardiac magnetic resonance (CMR) has become the gold standard technique for the assessment of RV structure and function. CMR also

From the *Imaging in Experimental Cardiology Laboratory, Centro Nacional de Investigaciones Cardiovasculares Carlos III (CNIC), Madrid, Spain; †Epidemiology, Atherothrombosis and Imaging Department, CNIC, Madrid, Spain; ‡Hospital Clínic, Institut d'Investigacions Biomèdiques August Pi i Sunyer, Barcelona, Spain; §Hospital Universitario Quirón Madrid, Universidad Europea de Madrid, Madrid, Spain; ‖Hospital Clínico San Carlos, Madrid, Spain; ¶Philips Healthcare Iberia, Madrid, Spain; #Hospital Puerta de Hierro, Madrid, Spain; **Facultad de Medicina, Universidad de Extremadura, Badajoz, Spain; ††Hospital Universitario Montepríncipe, Madrid, Spain; ‡‡Hospital Universitario Central de Asturias, Oviedo, Spain; and the §§Zena and Michael A. Wiener Cardiovascular Institute, Icahn School of Medicine at Mount Sinai, New York, New York. This study was partly funded by the "Red de Investigación Cardiovascular" (RIC) of the Spanish Ministry of Health (RD 12/0042/0054 to Dr. Ibáñez) and by ISCIII "Fondo de Investigación Sanitaria" grant PI13 /02339 to Dr. García-Álvarez. Drs. García-Álvarez, Mirelis, Fernández-Friera, Pizarro, and Ibáñez are members of different institutions participating in the RIC. Other sponsors were the Spanish Heart Foundation (basic research project 2012 to Dr. García-Álvarez) and a master research agreement between Philips Healthcare and CNIC. All authors have reported that they have no relationships relevant to the contents of this paper to disclose. The first 2 authors contributed equally to this work. Raymond Kwong, MD, MPH, has served as Guest Editor for this paper.

Manuscript received April 30, 2014; revised manuscript received August 26, 2014, accepted August 27, 2014.

allows evaluation of myocardial scarring after administration of gadolinium contrast agents. The presence of late gadolinium enhancement (LGE) at the RV insertion points is a common feature at advanced stages of chronic PH, correlating with poor RV performance and hemodynamic status. In recent years, T1 mapping by CMR has emerged as a noninvasive technique for the quantification of myocardial extracellular volume (ECV) in several diseases, holding the promise of early detection of myocardial involvement not detectable by LGE. Measurement of myocardial T1 times before and after a period of intravenous contrast infusion allows quantification of the equilibrium contrast extracellular volume (Eq-ECV) (1). Native (pre-contrast) T1 can also discriminate between normal myocardium and diffuse disease due to increased ECV and does not require contrast administration. ECV detected by noninvasive CMR is linked to poor prognosis in several cardiac diseases.

We assessed the hypothesis that in the early stages of chronic PH, before the onset of macroscopic fibrosis and thus LGE, CMR-measured ECV at the RV insertion points will be increased and correlate with PH-associated hemodynamic variables and RV performance. We tested this hypothesis in a prospective large-animal study of chronic PH using CMR myocardial T1 mapping (native T1 and Eq-ECV).

The study was approved by the Institutional Animal Research Committee and carried out in compliance with the Guide for the Care and Use of Laboratory Animals. Chronic PH was generated by surgical nonrestrictive banding of the main pulmonary vein (venous confluent arising from the junction of both inferior pulmonary veins) through a small thoracotomy in 38 Large White piglets (weight approximately 10 kg), as previously described (2). Our experience with this model is that restriction of flow and secondary PH arise progressively as the animal grows, reaching a mean pulmonary arterial pressure (PAP) of ≥25 mm Hg 2 months after surgery in most animals. Increase in PAP is associated with RV remodeling and typical pathological changes, including myocardial disarray and increased levels of interstitial collagen (2). A sham procedure was performed in 6 control animals, which underwent the same surgical procedure but without banding.

Two months after intervention, all animals underwent right heart catheterization immediately followed by CMR imaging. On the same day, a venous blood sample was collected to measure the hematocrit value for calculating Eq-ECV (1). All hemodynamic and CMR measures were obtained during spontaneous ventilation, anesthesia with intravenous midazolam at 0.2 mg/kg/h, and continuous electrocardiographic and oxymetric monitoring. A Swan-Ganz catheter was inserted through the femoral vein and positioned under fluoroscopy to measure PAP and cardiac output by thermodilution. Pulmonary vascular resistance (PVR) was calculated as the difference between mean PAP and the estimated left atrial pressure (left ventricular [LV] end-diastolic pressure measured with a pigtail catheter) divided by the cardiac output in Wood units. Cardiac output and PVR were also indexed by body surface area, estimated by the Brody formula. Established chronic PH was defined as a mean PAP of ≥25 mm Hg and borderline PH as a mean PAP of 21 to 24 mm Hg.

Immediately after right heart catheterization, animals were transferred to the CMR suite, adjacent to the catheterization laboratory. All CMR studies were performed using a 3.0-T TX Achieva system (Philips Healthcare, Best, the Netherlands). The detailed CMR acquisition protocol has been reported in detail elsewhere (2). Gadolinium contrast (gadopentetate dimeglumine, Bayer Healthcare Pharmaceuticals, Whippany, New Jersey) was administered at a dose of 0.1 mmol/kg for LGE sequence and 0.0011 mmol/kg/min for a 20-min infusion started after a 15-min delay for equilibrium contrast imaging, with a cumulative contrast dose of 0.122 mmol/kg (2). The T1 mapping sequence (modified Look-Locker inversion-recovery [MOLLI]) was acquired just before contrast administration and after equilibrium in a short-axis view at the level of the papillary muscles. All MOLLI sequences were based on a 3-5 scheme using a single-shot steady-state free precession readout sequence (repetition time/echo time/alpha 2.7 ms/1.36 ms/50°) with an in-plane acquisition resolution of 1.2×1.5 mm^2, inversion interval of 185 ms, half scan of 0.6, shot duration of 174 ms, and slice thickness of 8 mm. T1 maps were generated by nonlinear fitting of different inversion time points.

All CMR analyses were performed using specialized software (Extended MR Workspace, Philips Healthcare) in a blinded fashion. Pulmonary vein banding, performed with fabric tape, did not cause susceptibility artifacts and was not visible in the CMR sequences used in our study (Online Videos 1 and 2). Methodology for the analysis of cine and phase-contrast images has been described in detail previously (2). RV-arterial coupling—the ratio of PA effective elastance (Ea) to RV maximal end-systolic elastance (Emax) (Ea/Emax)—was estimated as

ABBREVIATIONS AND ACRONYMS

CMR = cardiac magnetic resonance

Ea = effective elastance

Emax = maximal end-systolic elastance

Eq-ECV = equilibrium contrast extracellular volume fraction

LGE = late gadolinium enhancement

LV = left ventricular

MOLLI = modified Look-Locker inversion-recovery

PAP = pulmonary arterial pressure

PH = pulmonary hypertension

PVR = pulmonary vascular resistance

ROI = region of interest

RV = right ventricular

RVEF = right ventricular ejection fraction

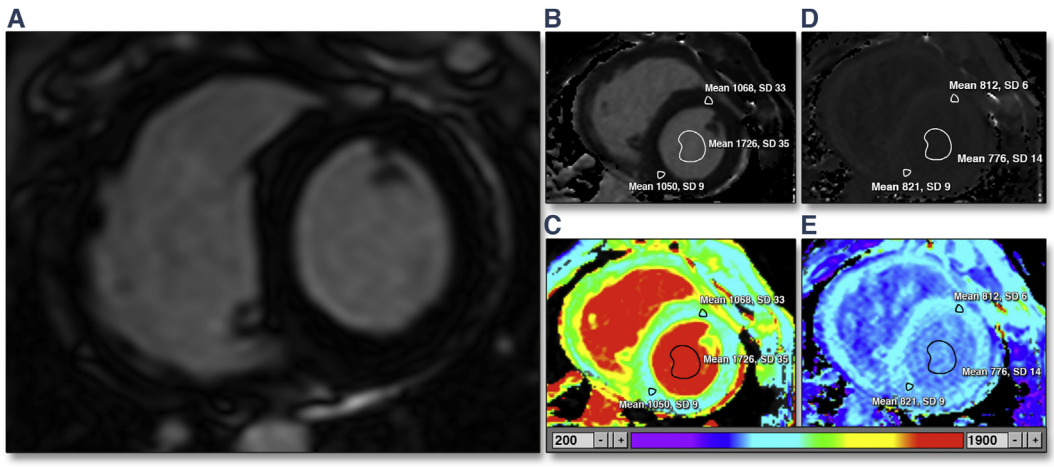

FIGURE 1 Representative T1 Maps From a Castrated Male Large-White Pig With Pulmonary Hypertension

Pulmonary hypertension was induced by surgical pulmonary vein banding. Panels show delayed enhancement **(A)** and T1 maps in a short-axis view of the heart at the level of the papillary muscles before contrast administration **(B and C)** and after equilibrium contrast **(D and E)**. Regions of interest are located at the anterior and inferior right ventricular insertion points and at the left ventricular blood pool. Online Videos 1 and 2.

([mean PAP – LV end-diastolic pressure]/RV stroke volume index/[mean PAP/RV end-systolic volume index]). Regions of interest (ROIs) were drawn on T1 maps in the myocardial anterior and inferior RV insertion points and LV cavity blood pool before contrast administration and after equilibrium (Figure 1). ROIs were additionally drawn in the septum and LV lateral wall for exploratory analysis. Special care was taken when ROIs were drawn to avoid tissue interface between myocardial and blood and thus partial volume averaging by blood contamination. T1 mapping images were acquired with high in-plane resolution to facilitate drawing the ROI inside the myocardium, and heart rate was updated before every MOLLI acquisition to define the correct trigger delay to minimize spatial misregistration. The ROIs were located at the same locations in all cases, independently of the presence of LGE. Native T1 values were obtained from the pre-contrast T1 map, and Eq-ECV values were calculated as previously described (1). Continuous variables are expressed as median (interquartile range). The distribution of the continuous variables was assessed using the Shapiro-Wilk test for normality. Comparisons of continuous variables between groups were performed using a Student unpaired *t* test (with Welch correction in case of heterogeneity of variances, as assessed by Levene test) or the Mann-Whitney *U* test, depending on whether or not they followed a normal distribution, respectively. When more than 2 groups were compared, the Wilcoxon test with Bonferroni correction was used for post-hoc comparisons. Correlations of T1 and Eq-ECV values with hemodynamic and CMR parameters were assessed using Pearson or Spearman correlation depending on the

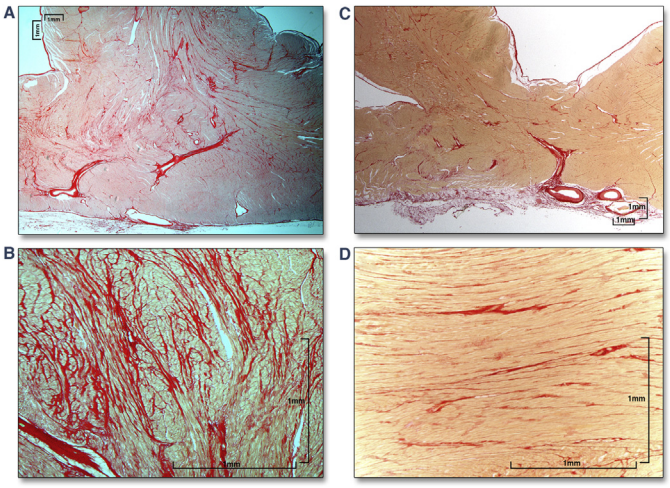

FIGURE 2 Picrosirius Red Staining of Cross Sections of the Heart

Banded animal **(A and B)** and sham-operated control **(C and D)**. Cross sections were taken at the level of the papillary muscles, focused on the inferior right ventricular insertion point. High magnification views clearly show increased interstitial collagen tissue (red) associated with myocardial disarray in the banded animal **(B)** versus that in the control **(D)**.

association type (linear or curvilinear) evaluated with scatterplots.

Morphometric analysis of the collagen network in myocardial RV insertion points was performed in 2 banded animals and 2 sham-operated controls using dedicated software (SigmaScan Pro 4.0, Jandel Scientific, San Rafael, California). Collagen was stained with picrosirius red, and staining was enhanced using polarizing light microscopy. We evaluated a minimum of 15 randomly chosen fields (10× magnification) in the anterior and inferior RV insertion points from each specimen, and values were averaged. In each field, a grid of vertical and horizontal lines was used, providing 121 intersection points. The proportion of connective tissue in each specimen, expressed as connective tissue density, was defined as the percentage of intersection points occupied by collagen.

The RV insertion points in banded animals showed increased interstitial collagen associated with fiber disarray (Figure 2). Morphometric analysis revealed that connective tissue density at the RV insertion points was significantly higher in banded animals compared with sham individuals (44.5 ± 5.5%; range 38.4% to 58.3% vs. 26.5 ± 7.5%; range 17.3% to 35.5%; $p < 0.05$).

Two months after surgery, banded animals had significantly higher PAP, PVR, PA dimensions, and RV end-systolic volume than sham-operated controls and had lower weight, arterial oxygen saturation, RV ejection fraction (RVEF), and CMR-quantified cardiac index (Table 1). There were no significant differences in heart rate, systemic blood pressure, LV mass, LV volumes, or LV ejection fraction. Banded animals showed higher native T1 and Eq-ECV values at the anterior and inferior RV insertion points, and T1 mapping values at the RV insertion points in banded animals were significantly higher than those in the LV lateral wall and septum (Table 1).

Native T1 times and Eq-ECV at the anterior and inferior RV insertion points correlated with pulmonary hemodynamics, RV volumes, RVEF, PA area, and estimated Ea/Emax (Figure 3). We observed similar correlations for the anterior and inferior RV insertion points. Eq-ECV, but not native T1, showed a significant positive correlation with the RV mass index and an inverse correlation with PA elasticity (R between 0.39 and 0.47; $p < 0.05$). Correlations did not differ significantly when heart rate was included in the model as a covariate or when the analysis was restricted to banded animals (data not shown).

LGE was present in both RV insertion points of 4 animals (10.5%). These 4 animals had more severe PH than banded animals without LGE, with significantly higher mean PAP (median [interquartile range] 62.5 [4.8] mm Hg vs. 33 [9.5] mm Hg) and PVR index (16.9 [12.7] Wood units/m^2 vs. 6.3 [3.3] Wood units/m^2) and significantly lower RVEF (45.8% [13.0%] vs. 53.5% [8.6%]). Native T1 at both RV insertion points was also significantly higher in these animals compared with banded animals without LGE: 1,153 (154) versus 1,008 (90) ms at the anterior insertion point and 1,121 (160) versus 994 (83) ms at the inferior RV insertion point, respectively ($p < 0.05$). Similarly, Eq-ECV was larger: 44.0% (14.3%) versus 34.0% (10.3%) and 43.0% (10.8%) versus 34.5% (9.5%) at the same locations

TABLE 1 Population Hemodynamic and CMR Characteristics

	Sham (n = 6)	Banding (n = 38)	p Value
Morphometric and hemodynamic			
Weight, kg	44.8 (10.4)	33.5 (14.1)	0.015
Arterial oxygen saturation, %	93.0 (4.0)	88.0 (13.0)	0.002
Heart rate, beats/min	78.0 (15.0)	74.5 (24.0)	0.240
Systolic systemic BP, mm Hg	118.5 (17.0)	114.0 (18.0)	0.437
Systolic PAP, mm Hg	28.0 (4.5)	44.5 (22.3)	<0.001
Mean PAP, mm Hg	21.5 (4.0)	33.5 (13.8)	<0.001
Cardiac index, l/min/m^2	4.5 (0.8)	4.0 (1.1)	0.181
LV end-diastolic pressure, mm Hg	7.0 (4.0)	9.0 (3.0)	0.149
PVR, Wood units	3.1 (1.2)	7.3 (6.3)	<0.001
PVR index, Wood units/m^2	3.2 (1.5)	6.4 (4.3)	<0.001
Hematocrit, %	33.2 (4.5)	33.0 (5.5)	0.803
CMR measures			
RVEDV index, ml/m^2	89.5 (17.6)	97.7 (28.9)	0.056
RVESV index, ml/m^2	33.0 (8.6)	41.7 (15.7)	0.006
RV mass index, g/m^2	18.4 (3.6)	23.5 (10.2)	0.108
RVEF, %	61.9 (6.3)	51.9 (8.8)	0.005
LVEDV index, ml/m^2	94.9 (11.9)	90.2 (13.8)	0.098
LVESV index, ml/m^2	39.7 (9.2)	36.2 (9.8)	0.091
LV mass index, ml/m^2	48.1 (19.5)	50.2 (9.9)	0.960
LVEF, %	56.7 (6.2)	58.5 (6.2)	0.374
PA maximal area, cm^2/m^2	6.4 (1.3)	7.4 (2.5)	0.036
PA minimal area, cm^2/m^2	4.3 (1.3)	5.6 (2.2)	0.020
RV cardiac index, l/min/m^2	4.4 (0.8)	4.1 (0.5)	0.022
PA elasticity, %	36.8 (18.0)	32.9 (20.0)	0.122
Ea/Emax	0.37 (0.21)	0.62 (0.39)	0.004
T1 value at the anterior RVIP, ms	973 (104)	1,011 (87)	0.052
T1 value at the inferior RVIP, ms	963 (110)	996 (101)	0.004
T1 value at the septum, ms	939 (101)	971 (74)	0.305
T1 value at the LV lateral wall, ms	953 (197)	972 (78)	0.472
ECV at the anterior RVIP, %	25.5 (5.0)	35.0 (11.0)	<0.001
ECV at the inferior RVIP, %	25.0 (5.0)	37.0 (9.8)	<0.001
ECV value at the septum, %	24.0 (10.0)	27.0 (11.0)	0.074
ECV value at the LV lateral wall, %	26.0 (8.7)	29.5 (9.3)	0.328

Values are median (interquartile range).

BP = blood pressure; CMR = cardiac magnetic resonance; Ea = effective elastase; Emax = maximal end-systolic elastance; ECV = equilibrium contrast extracellular volume; LV = left ventricular; LVEF = left ventricular ejection fraction; LVEDV = left ventricular end-diastolic volume; LVESV = left ventricular end-systolic volume; PA = pulmonary artery; PAP = pulmonary arterial pressure; PVR = pulmonary vascular resistance; RV = right ventricular; RVEDV = right ventricular end-diastolic volume; RVEF = right ventricular ejection fraction; RVESV = right ventricular end-systolic volume; RVIP = right ventricular insertion point.

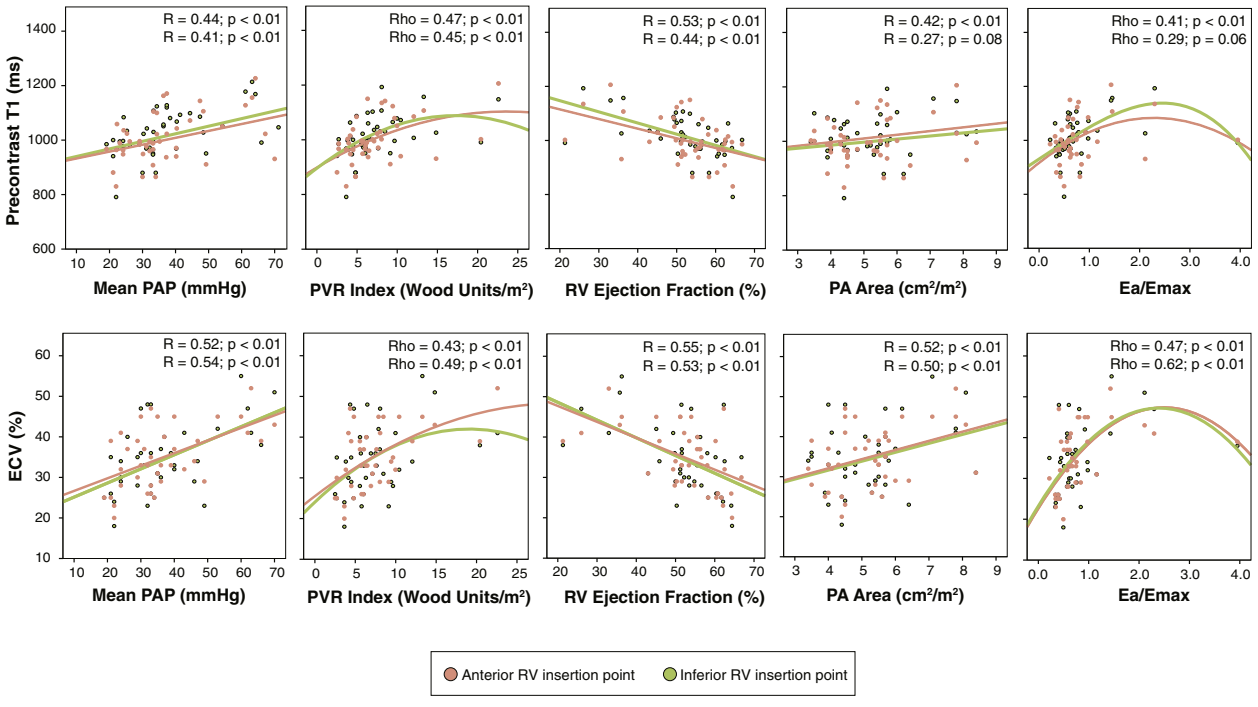

FIGURE 3 Correlation of T1 Mapping Parameters With Hemodynamics and RV Performance

Scatter plots show the association of native T1 and equilibrium contrast extracellular volume (Eq-ECV) values at the right ventricular (RV) insertion points with mean pulmonary arterial pressure (PAP), pulmonary vascular resistance (PVR) index, RV ejection fraction, pulmonary artery (PA) area, and ventricular-arterial coupling (Ea/Emax). Lines of best fit were drawn using linear or quadratic adjustment depending on the association type (linear or curvilinear).

($p < 0.05$). After these 4 cases were excluded from the analysis, native T1 and Eq-ECV remained significantly higher in banded animals compared with sham-operated controls and was significantly associated with PVR, RVEF, RV end-systolic volume, and RV-arterial coupling (data not shown).

LGE appears as the result of delayed clearance of gadolinium from an expanded ECV that can be the result of fibrillar deposits, fibrosis, or necrosis. Independent of the cause of myocardial scarring, the presence of LGE indicates poor prognosis in all investigated cardiac diseases. In chronic PH, LGE at the RV insertion points has been widely described, with increasing prevalence correlating with the severity and duration of the disease and showing an inverse association with RV performance. However, the prognostic significance of LGE in patients with PH is not completely established. T1 mapping characterization is an emerging technology that allows early detection of ECV expansion. There are several methods for ECV estimation, Eq-ECV being the most validated. Native T1 mapping is particularly attractive in this regard because it does not require administration of a contrast agent. To our knowledge, this is the first study on T1 mapping applied to chronic PH. The use of a controlled experimental animal model of chronic PH avoids confounding by factors such as medication, comorbidities, age, sex, or disease duration, all of which can affect T1 mapping parameters. CMR acquisition immediately after hemodynamic assessment further strengthens the associations observed. We focused on the second month after surgery because this time coincides with the development of PH in our pig model, and we wanted to study the early stages of the disease, before the onset of LGE.

T1 mapping evaluation based on drawing myocardial ROIs makes it difficult to directly interrogate the RV free wall, even in the presence of RV hypertrophy. Evaluation of the interventricular septum (frequently done in other cardiomyopathies) has the inconvenience of septal bowing, frequently observed in these patients. Conversely, placing an ROI at the RV insertion points is simple and reproducible. In addition, LGE is known to appear earlier in these areas than in the septum. In fact, in our banded

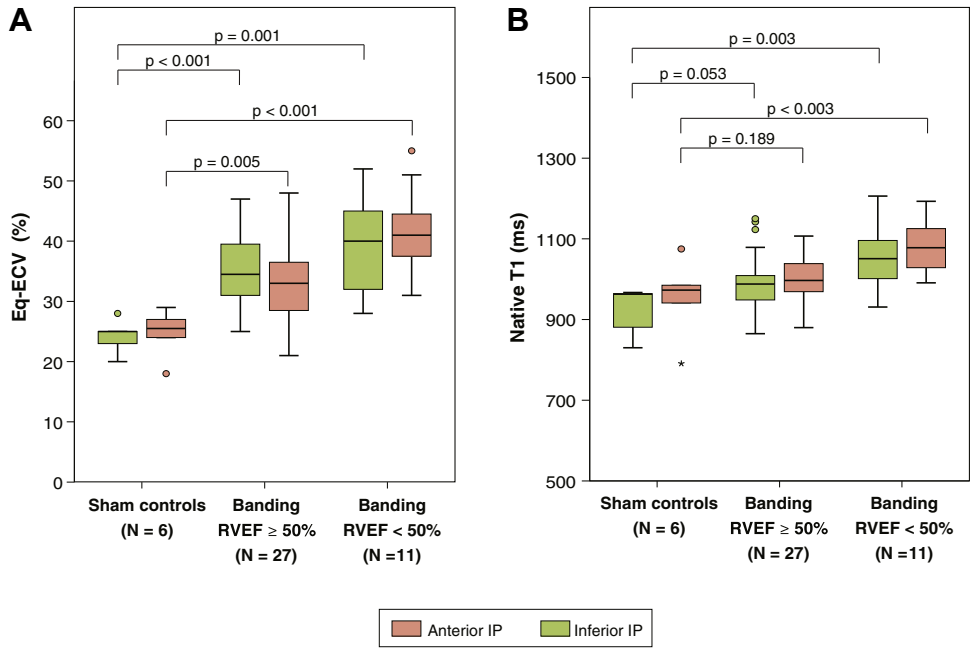

FIGURE 4 **Values for Eq-ECV and Native T1**

(A) Eq-ECV. **(B)** Native T1 at RV insertion points grouped according to RV systolic function. Box plots represent median and first to third quartiles. IP = insertion point; RVEF = right ventricular ejection fraction; other abbreviations as in Figure 3.

animals, T1 and Eq-ECV values were clearly higher at the RV insertion points compared with the septum and LV lateral wall.

Of 38 banded animals, 33 had established chronic PH and 5 had borderline PH (with confirmed established PH 1 month later). Animals with either established or borderline chronic PH had significantly higher Eq-ECV at the RV insertion points compared with sham-operated controls (established PH 36.0% [12.0%], borderline PH 34.0% [5.0%], and sham-operated 24.0% [5.0%] for the anterior insertion point and 37.0% [12.0%], 39.0% [5.0%], and 25.0% [5.0%] for the same conditions at the inferior RV insertion point). The native T1 values showed a similar trend, although differences between borderline PH and sham groups did not reach statistical significance (1,022 [105] ms, 1,000 [42] ms, and 973 [104] ms for the anterior RV insertion point; and 1,010 [127] ms, 1,003 [58] ms, and 963 [110] ms for the inferior RV insertion point in established PH, borderline PH, and sham groups, respectively).

Consistent with these findings, although 27 banded animals had normal RVEF and 11 had RV dysfunction (RVEF <50%), banded animals with normal RVEF had significantly higher Eq-ECV at both RV insertion points compared with sham-operated controls (Figure 4A). In contrast, differences in native T1 values between banded animals with normal RVEF and sham-operated controls did not reach statistical significance (Figure 4B).

Eq-ECV thus appeared to be more sensitive in this setting than native T1 because associations with early manifestations of PH (PA elasticity and arterial-RV coupling) were stronger and it discriminated between animals with incipient PH and sham-operated animals; however, this assumption requires further investigation. Interestingly, a recent study evaluating several T1 mapping approaches also found Eq-ECV to be superior to native T1 in terms of reproducibility and ability to differentiate disease from health.

In the present study, measurement was more feasible at the anterior RV insertion point, whereas interobserver concordance and association with PH hemodynamics and RV performance were slightly superior for the inferior RV insertion point. We were able to evaluate native T1 and Eq-ECV at the anterior RV insertion point in all cases. In contrast, at the inferior RV insertion point, native T1 could not be measured in 1 case and Eq-ECV measurement

JACC: CARDIOVASCULAR IMAGING, VOL. 8, NO. 1, 2015
JANUARY 2015:76–82

was not possible in 5 cases (11%) due to suboptimal quality of the post-equilibrium acquisition. Intraclass correlation coefficients (95% confidence interval) for interobserver concordance were 0.87 (0.48 to 0.97) and 0.89 (0.57 to 0.98) for native T1 at the anterior and inferior RV insertion points, respectively, and 0.83 (0.42 to 0.96) and 0.90 (0.59 to 0.98) for Eq-ECV. Mean bias ± SD of the differences was 12.25 ± 18.5 ms for anterior native T1, 6.5 ± 23.4 ms for inferior native T1, −1.8 ± 5.9 for anterior Eq-ECV, and 0.7 ± 4.8 for inferior Eq-ECV. Interestingly, LGE has been reported to occur more frequently at the inferior insertion point. However, the inferior wall is more affected by susceptibility artifacts generated by the heart-pulmonary interface, which may explain the lower feasibility of T1 measurements at this location.

STUDY LIMITATIONS. Histological evaluation was not performed in all cases, precluding assessment of the association between collagen density and T1 values. Nevertheless, this association has been repeatedly demonstrated in other scenarios (1), and our PH experimental model showed a significant increase in collagen density at the RV insertion points. A flip angle of 50°, rather than the conventional 35°, was used to compensate for the small pixel size derived from the high spatial resolution used. Nevertheless, previous studies comparing both flip angles reported only a small underestimation of T1 values (<1%) with a 50° flip angle for the range of values found in our study (700 to 1,200 ms). The T1 values observed in our study were lower than those reported for 3-T in the literature. This difference might reflect several factors. Heart rate in our cohort (median 77 beats/min; range 55 to 107 beats/min) was slightly higher than that reported for patients studied in other conditions. However, there was not a statistically significant correlation between heart rate and T1 mapping parameters, with the exception of native T1 at the inferior RV insertion point, which showed a mild correlation ($R = -0.34$; $p = 0.024$); all other p values were >0.28. Nevertheless, to rule out a potential confounding effect, heart rate was included as a covariable in a sensitivity analysis. Other potential factors that might have affected our results are interspecies differences (pigs instead of humans), hormones (castrated males), young age (3 months old), and body size, all of which could influence T1 values. Clinical validation in patients with PH will therefore be necessary to confirm our results.

CONCLUSIONS

The current study demonstrated that CMR-measured native T1 and Eq-ECV at the RV insertion points increased in early stages of chronic PH and correlated with hemodynamics and RV dysfunction in an experimental porcine model of chronic PH.

ACKNOWLEDGMENTS The authors thank Gonzalo J. Lopez, Angel Macias, and Braulio Pérez for high-quality CMR examinations; Tamara Córdoba, Oscar Sanz, Eugenio Fernández, and the rest of the team at the CNIC farm and Comparative Medicine Unit for outstanding animal care and support; and Simon Bartlett (CNIC) for English editing.

REPRINT REQUESTS AND CORRESPONDENCE: Dr. Borja Ibáñez or Dr. Ana García-Álvarez, Epidemiology, Atherothrombosis and Imaging Department, Centro Nacional de Investigaciones Cardiovasculares Carlos III, Melchor Fernández Almagro 3, 28029 Madrid, Spain. E-mail: bibanez@cnic.es OR ana.garcia@cnic.es; anagarci@clinic.ub.es

REFERENCES

1. Flett AS, Hayward MP, Ashworth MT, et al. Equilibrium contrast cardiovascular magnetic resonance for the measurement of diffuse myocardial fibrosis: preliminary validation in humans. Circulation 2010;122:138–44.

2. García-Álvarez A, Fernández-Friera L, García-Ruiz JM, et al. Noninvasive monitoring of serial changes in pulmonary vascular resistance and acute vasodilator testing using cardiac magnetic resonance. J Am Coll Cardiol 2013;62:1621–31.

KEY WORDS equilibrium contrast, extracellular volume, magnetic resonance, native T1, pulmonary hypertension, T1 mapping

APPENDIX For supplemental videos and their legends, please see the online version of this article.